

Interparticle interactions in coupled Au–Fe₃O₄ nanoparticles

N. A. Frey,¹ M. H. Phan,¹ H. Srikanth,^{1,a)} S. Srinath,² C. Wang,³ and S. Sun³

¹*Department of Physics, University of South Florida, Tampa, Florida 33620, USA*

²*School of Physics, University of Hyderabad, Hyderabad 500046, India*

³*Department of Chemistry, Brown University, Providence, Rhode Island 02912, USA*

(Presented 13 November 2008; received 14 September 2008; accepted 14 October 2008; published online 2 February 2009)

Complex ac susceptibility measurements are reported on composite Au–Fe₃O₄ nanoparticles of two different configurations—the so-called “dumbbell” and “flower” configurations. The frequency-dependent blocking temperature was fitted to two separate models in an attempt to understand the relaxation and the role of interactions present in the nanoparticle arrays. While the Néel–Arrhenius model failed to accurately describe the blocking behavior of both types of particles, the Vogel–Fulcher model was shown to fit the dumbbell particles indicating the importance of weak interparticle interactions in this system. The flower nanoparticles, however, failed to yield physical fit parameters for both models, indicating that the interactions present in these particles are not solely dipolar but likely associated with competing intraparticle interactions. Radio-frequency transverse susceptibility measurements also confirm these features. © 2009 American Institute of Physics. [DOI: 10.1063/1.3056582]

Collective magnetic behavior in nanoparticle arrays is an important current topic as it can be very important for magnetic storage and biomedical applications.¹ However, a good understanding requires systematic static and dynamic magnetization studies as the collective behavior results from the competing contributions of surface and finite-size effects, interparticle interactions, and the random distribution of anisotropy axes throughout the system.^{1–5} While in single nanoparticle systems (e.g., uncoated spherical Fe₃O₄ nanoparticles) interparticle dipolar interactions have been shown to dominantly affect the relaxation behavior and result in particle agglomeration causing the nanoparticles to no longer be magnetically isolated,^{1,5} the situation may become more complex in systems in which magnetic particles are coupled with other nonmagnetic particles (namely, composite nanoparticles) such as the dumbbell- and flowerlike Au–Fe₃O₄ nanoparticles recently synthesized by the Brown group.^{6,7} Here the dumbbell nanoparticles consist of one Fe₃O₄ nanoparticle grown epitaxially onto one facet of an Au seed particle, whereas the flower nanoparticles consist of several Fe₃O₄ particles grown epitaxially onto multiple facets of an Au seed particle.⁸

In this paper, we report on a comparative study of the dynamic susceptibility at ac and radio frequencies (rf) in composite Au–Fe₃O₄ nanoparticles. Our results indicate that weak dipolar interactions are present in the dumbbell nanoparticles, but competing intraparticle interactions are possibly dominant in the flower nanoparticles.

Synthesis of the dumbbell Au–Fe₃O₄ nanoparticles consisted of decomposition of iron pentacarbonyl [Fe(CO)₅] over the surface of already synthesized Au seed particles in the presence of surfactants followed by oxidation in air. By changing the solvent of the reaction from a nonpolar hydro-

carbon to a slightly polarized solvent (e.g., diphenyl ether), multiple nucleation sites become available for the Fe₃O₄ onto the Au, and the result is the flower structure. The nanoparticles were structurally characterized using x-ray diffraction, transmission electron microscopy (TEM), and high resolution TEM and presented in extensive detail elsewhere.⁸ Magnetic measurements were done using a commercial physical properties measurement system (PPMS) from Quantum Design. In phase (χ') and out of phase (χ'') susceptibility measurements were performed in an ac magnetic field of 10 Oe over a wide range of frequencies between 10 Hz and 10 kHz. The samples studied in this work were in the form of dried powder.

Figures 1(a) and 1(b) show χ' and χ'' , respectively, as a function of temperature for the dumbbell nanoparticles, while Figs. 1(c) and 1(d) show the same for the flower nanoparticles with insets showing TEM images of the dumbbell and flower particles, respectively. For both types of particles, it can be seen that the peak associated with the blocking transition increases in temperature with increase in frequency, consistent with typical nanoparticle behavior.^{4,5} For the dumbbell nanoparticles, the χ' peak decreases in magnitude with increase in frequency while the χ'' peak increases with frequency. This feature is similar to that observed in bare Fe₃O₄ nanoparticles.⁵ The flower particles, however, show a decrease in magnitude in both χ' and χ'' with increase in frequency. This type of behavior has previously been reported in spin-frustrated systems⁹ giving a first indication that the interactions involved in the flower nanoparticles are more complex in nature than in the dumbbell nanoparticles.

To investigate the frequency-dependent blocking temperature in the context of interparticle interactions, we plotted blocking temperature versus $\ln(f)$ and first tried to fit the χ' data to the Néel–Arrhenius (NA) model, which describes

^{a)}Author to whom correspondence should be addressed. Electronic mail: sharihar@cas.usf.edu.

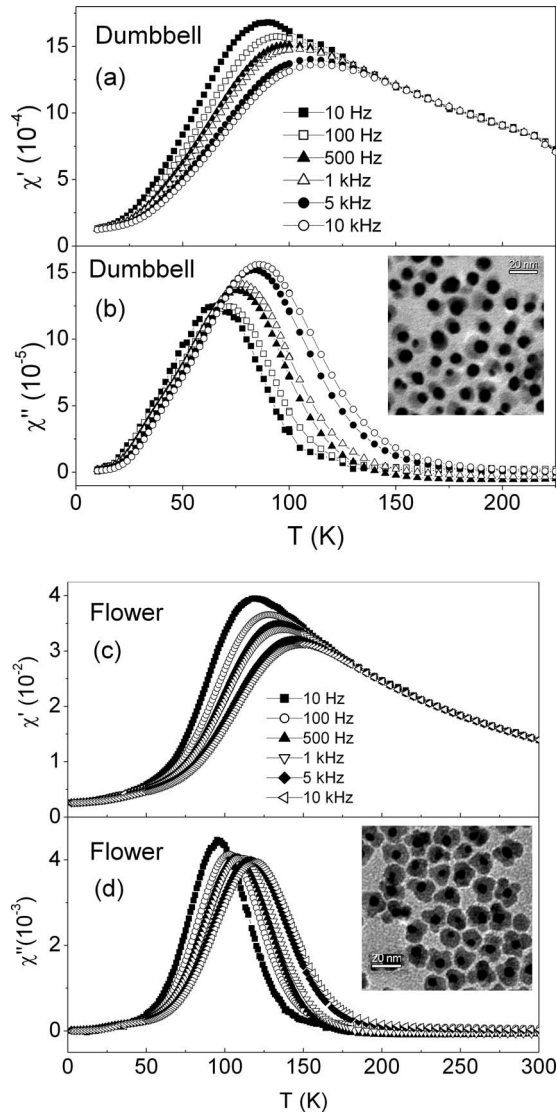


FIG. 1. In phase and out of phase ac susceptibility as a function of temperature at different frequencies for the dumbbell [(a) and (b)] and flower [(c) and (d)] Au–Fe₃O₄ nanoparticles. Insets show the TEM images of each type of particles.

the frequency dependence for an array of noninteracting single domain particles,

$$\ln(f) = \ln(f_0) - E_a/k_B T, \quad (1)$$

where E_a is the activation energy, k_B is the Boltzmann constant, and T is the temperature. The values obtained for the Larmor frequency and activation energy for the dumbbell particles were $f_0 = 3.2 \times 10^{14}$ Hz and $E_a = 2527$ K, respectively, while for the flower nanoparticles the fits yielded $f_0 = 2.2 \times 10^{16}$ Hz and $E_a = 4231$ K, respectively. Since the accepted values for the Larmor frequency fall in the range of 10^9 – 10^{13} Hz, it was determined that the NA model did not accurately describe either of these systems and that the interaction effects are important.^{10,11}

The Vogel–Fulcher (VF) model, which is used to account for weak dipolar interactions in nanoparticle arrays, was then fitted to the χ' data in an attempt to explain the deviation from the NA model. Figure 2 shows the T_B values plotted against $\ln(f)$ for both types of particles along with fits

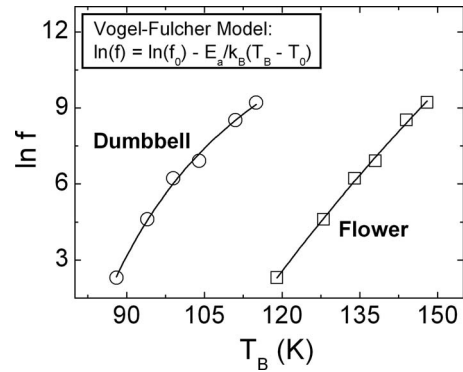


FIG. 2. T_B as a function of frequency for dumbbell and flower Au–Fe₃O₄. The solid lines are the fits to Eq. (2)—the VF model.

to the VF model. The VF model is a modification of the NA model which includes the addition of another term, T_0 , which describes the energy scale of the dipolar interactions and is expressed as

$$\ln(f) = \ln(f_0) - E_a/k_B(T - T_0). \quad (2)$$

The data when fitted to the VF model yielded f_0 , E_a/k_B , and T_0 values of 1.3×10^8 Hz, 616 K, and 50 K, respectively, for the dumbbell particles. These values are all physically reasonable, and we thus conclude that the VF model validates the presence of weak interparticle interactions in this system.^{10,11} The flower nanoparticles, on the other hand, did not yield physical values when fitted to the VF model, and we obtained f_0 , E_a/k_B , and T_0 values of 2.7×10^{27} Hz, 13 675 K, and -105 K. These values indicate the VF model fails to describe the interactions that are present in this system and points to a more complex situation. Given that the flower particles have a complex geometry due to the clustering of multiple magnetic nanoparticles to the seed Au particle, the failure of both NA and VF models is not particularly surprising.

Note that in this study, we have focused on a comparison of the results in dumbbell and flower nanoparticle samples in the dried powder form. The strength of the interparticle interactions can be best explored through systematic studies with samples containing different concentrations of the nanoparticles embedded in a medium such as paraffin wax, thereby tuning the mean interparticle separation. These experiments are currently under way and a complete study of the dc, ac, and rf susceptibilities under these conditions would be reported in a future publication.

To independently check this from a different perspective, we measured the transverse susceptibility (TS) of both types of particles using a rf tunnel diode oscillator integrated into the PPMS.⁶ Here TS, which refers to the magnetic susceptibility in one direction as a function of applied dc field in the transverse direction, is a direct probe of the magnetic anisotropy of the material as peaks are seen at the positive and negative anisotropy fields for a material.^{6,12} Aharoni *et al.*¹³ theorized that the TS for a Stoner–Wohlfarth particle with its hard magnetic axis aligned with the dc field should yield peaks at the anisotropy fields and switching fields as the dc field is swept from positive to negative saturation. However, we have experimentally shown that for an array of nanopar-

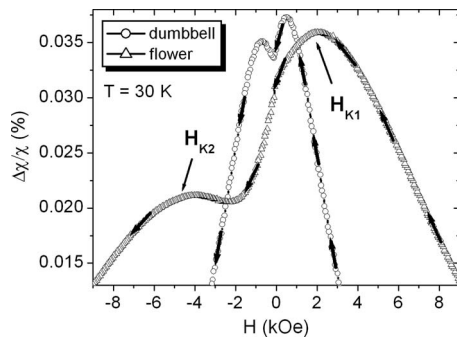


FIG. 3. TS scans of the dumbbell (circles) and flower (triangles) Au–Fe₃O₄ nanoparticles taken at 30 K.

ticles with a distribution in size, the switching peak is often merged with one of the anisotropy peaks and a marked asymmetry in both peak location heights can be seen.^{6,14} In the present case, there is a striking difference in peak height and location symmetry between the dumbbell and flower nanoparticles, as shown in Fig. 3. In the dumbbell nanoparticles, the peaks not only appear at much smaller fields (consistent with a lower effective anisotropy) but also are much closer to each other in height and field location. This behavior of TS, together with the ac susceptibility [Figs. 1(a) and 1(b)] and dc magnetization data,⁶ indicates that the interactions present in the dumbbell particles are weak interparticle interactions.

The interactions in the flower particles are more complex and are not accounted by interparticle interactions alone. Because of the cluster geometry of individual flower particles, direct and indirect exchange couplings between the component particles are likely along with other interface effects mediated by the Au seed particle. The extremely large asymmetry of the TS peaks for the flower nanoparticles can in general be reconciled with the fact that each flower particle is a compact cluster of Fe₃O₄ particles bound to a single Au particle, thus forming a geometry favoring a certain level of short-range interactions between the spins. For this system, the χ'' data [Figs. 1(c) and 1(d)] clearly suggest features consistent with geometric/spin frustration being present, likely arising due to the *intraparticle* interactions present between Fe₃O₄ particles sharing the same Au seed particle. Whether or not these interactions are solely a proximity effect is unclear, but the results published on other systems indicate that robust exchange type coupling mediated a nonmagnetic metal is possible.¹⁵

The combination of spin frustration present due to nearby Fe₃O₄ particles sharing the same Au seed particle and

the coupling of adjacent Fe₃O₄ particles mediated by the Au sets up competing intraparticle interactions that likely dominate over any interparticle interactions present. This unusual behavior associated with the cluster-type geometry of Au and Fe₃O₄ clearly does not fit either NA or VF models and prompts a need for further understanding of intraparticle interactions within composite nanoparticles.

In summary, we have performed ac susceptibility and rf TS measurements on dumbbell- and flowerlike Au–Fe₃O₄ nanoparticles. While the behavior of the dumbbell-like nanoparticles can be explained by weak interparticle interactions, the flowerlike nanoparticles exhibit much more complex behavior, likely associated with competing intraparticle interactions.

Work at USF supported by DOE through Grant No. DE-FG02-07ER46438. H.S. also acknowledges support from the Center for Integrated Functional Materials through DoD-USAMRMC Grant No. W81XWH-07-1-0708. Work done at Brown was supported through NSF Grant No. DMR 0606264.

¹M. Blanco-Mantecon and K. O'Grady, *J. Magn. Magn. Mater.* **296**, 124 (2006).

²W. Luo, S. R. Nagel, T. F. Rosenbaum, and R. E. Rosensweig, *Phys. Rev. Lett.* **67**, 2721 (1991).

³K. Jonason, E. Vincent, J. Hamann, J. P. Bouchaud, and P. Nordblad, *Phys. Rev. Lett.* **81**, 3243 (1998).

⁴C. Djurberg, P. Svedlindh, P. Nordblad, M. F. Hansen, F. Bodker, and S. Morup, *Phys. Rev. Lett.* **79**, 5154 (1997).

⁵G. F. Goya, T. S. Berquó, F. C. Fonseca, and M. P. Morales, *J. Appl. Phys.* **94**, 3520 (2003).

⁶N. A. Frey, S. Srinath, H. Srikanth, C. Wang, and S. Sun, *IEEE Trans. Magn.* **46**, 3094 (2007).

⁷C. Xu, J. Xie, D. Ho, C. Wang, N. Kohler, E. G. Walsh, J. R. Morgan, Y. E. Chin, and S. Sun, *Angew. Chem.* **47**, 173 (2007).

⁸H. Yu, M. Chen, P. M. Rice, S. X. Wang, R. L. White, and S. Sun, *Nano Lett.* **5**, 379 (2005).

⁹D. N. H. Nam, R. Mathieu, P. Nordblad, N. V. Khiem, and N. X. Phuc, *Phys. Rev. B* **62**, 1027 (2000).

¹⁰H. Shim, A. Manivannan, M. S. Seehra, K. M. Reddy, and A. Punnoose, *J. Appl. Phys.* **99**, 08Q503 (2006).

¹¹J. Zhang, C. Boyd, and W. Luo, *Phys. Rev. Lett.* **77**, 390 (1996).

¹²N. A. Frey, S. Srinath, H. Srikanth, M. Varela, S. Pennycook, G. Miao, and A. Gupta, *Phys. Rev. B* **74**, 024420 (2006).

¹³A. Aharoni, E. H. Frei, S. Shtrikman, and D. Treves, *Bull. Res. Council. Isr., Sect. F* **6**, 215 (1957).

¹⁴P. Poddar, M. B. Morales, N. A. Frey, S. A. Morrison, E. E. Carpenter, and H. Srikanth, *J. Appl. Phys.* **104**, 063901 (2008).

¹⁵J. P. Pierce, M. A. Torija, Z. Gai, J. Shi, T. C. Schulthess, G. A. Farnan, J. F. Wendelken, E. W. Plummer, and J. Shen, *Phys. Rev. Lett.* **92**, 237201 (2004).